Unstaggered Central Schemes for Arrhenius-type Look-ahead Traffic Flow Model

Said Belkadi, Mohamed Atounti, Zakaria El Allali

***Abstract*—We consider an unstaggered central scheme based on the staggered Lax-Friedrichs scheme to solve a non-local traffic flow model with an Arrhenius-type look-ahead rule. Our model appears in the form of a scalar non-local conservation law. The method produces a nonoscillatory numerical solution on a single grid, avoiding the highly detailed Riemann problem-solving process that arises at the cell boundaries. It is second-order accurate. Additionally, to achieve the desired second-order accuracy, the convolution term in each cell is evaluated using piecewise linear reconstruction. It then evaluates the gradient by ensuring non-oscillatory nature reconstruction using a non-linear limiter. The obtained numerical results are in good agreement with the data reported in the current literature, thus assessing the accuracy and ease of application of the new method.**

***Index Terms*—Finite volume methods, Traffic flow models, Nonlocal conservation laws, Limiters.**

I. Introduction

TRAFFIC flow modeling is currently a subject of active investigation in the field of research. The impetus behind these is the imperative to comprehend and forecast the intricate dynamics of vehicular traffic. Accurate traffic simulations are unquestionably critical for road infrastructure design [12], urban planning, and congestion management strategies [6]. However, conventional, macroscopic models of traffic flow, such as the Lighthill-Whitham-Richards (LWR) model [11], typically fail to consider the emergent behaviors and interfused interactions that exist in real-world traffic scenarios. Despite this, these models have provided profound insights.

In recent years, the models describing drivers have been developed toward more sophisticated ones, including nonlocal effects and reproducing the realistic behaviors of drivers. One of these developments is introducing the so-called look-ahead Arrhenius-type model that defines drivers' anticipation of conditions ahead [16]. This is because the rule considers empirical observations that show that, as vehicle density increases, the traffic flux exhibits complex, right-skewed behavior rather than being purely concave or symmetric [8].

The creation of reliable numerical schemes to roughly solve issues arising in traffic flow models has been an extremely active and ongoing process. The authors of [3], [5], [9] devised a second-order central scheme to approximate the solution of nonlocal traffic flow models. The plan can be seen as a logical progression from the second-order central scheme of Nessyahu and Tadmor (NT) [15] and the staggered Lax-Friedrichs (LxF) scheme. The NT scheme alternates between the staggered dual grid and the original grid at successive time steps [14], avoiding the solution of Riemann issues at cell interfaces. The numerical solution, which is piecewise linear and specified at the centers of the control cells, assures second-order accuracy in space. Additionally, the use of slope-limiting ensures an oscillation-free numerical solution.

This paper aims to develop an unstaggered central scheme (UCS) specifically for the numerical solution of nonlocal conservation laws governing Arrhenius-type look-ahead rules in traffic flow models. This new UCS method represents a significant advancement over previous approaches [1], [2], [13], [14], as it extends and generalizes the well-established Nessyahu-Tadmor (NT) staggered central scheme and the unstaggered adaptation proposed by Jiang et al. [7], incorporating the Arrhenius-type look-ahead distance formulation.

A key distinguishing feature of the UCS is its ability to evolve the numerical solution on a single computational grid, eliminating the need for staggered grids employed in earlier methods. This streamlined approach simplifies the computational process and has the potential to enhance computational efficiency by avoiding the complexities associated with alternating between staggered grids at successive time steps. To circumvent the need for solving Riemann problems at cell interfaces, a critical challenge in numerical schemes for hyperbolic conservation laws, the UCS ingeniously employs an implicit "ghost" staggered grid layer. This innovative technique allows the scheme to leverage the benefits of staggered grids without explicitly computing the solution on multiple grids.

Furthermore, the UCS employs a piecewise linear reconstruction of the numerical solution, ensuring that the scheme maintains second-order accuracy in both space and time. This high-order accuracy is a desirable property inherited from the original NT scheme and is crucial for capturing the intricate dynamics of traffic flow accurately.

The paper substantiates the performance and accuracy of the proposed UCS through several numerical experiments, demonstrating its ability to effectively solve nonlocal traffic flow models while retaining the desirable properties of the NT scheme and overcoming its limitations related to staggered grids.

The remainder of the paper is structured as follows: Section 2 introduces the nonlocal traffic flow model with Arrhenius-type look-ahead rules, which serve as the governing equation for the numerical simulations. The formulation of the novel unstaggered, finite volume one-dimensional scheme is detailed in Section 3, where we elucidate the main aspects of our approach, including the implicit "ghost"

Manuscript received May 17, 2024; revised November 15, 2024.

Said. Belkadi is a researcher at the Department of Mathematics, Multidisciplinary Faculty of Nador, University Mohamed First, Oujda, Morocco. (e-mail: s.belkadi.said@gmail.com).

Mohamed. Atounti is a professor at the Department of Mathematics, Multidisciplinary Faculty of Nador, University Mohamed First, Oujda, Morocco. (e-mail: atounti@hotmail.fr).

Zakaria. El Allali is a professor at the Department of Mathematics, Multidisciplinary Faculty of Nador, University Mohamed First, Oujda, Morocco. (e-mail: z.elalli@ump.ac.ma).

staggered grid and the piecewise linear reconstruction of the numerical solution. Section 4 then presents and analyzes the numerical results from various test cases, showcasing the accuracy, convergence, and performance of the proposed unstaggered central scheme in solving the nonlocal traffic flow model. Finally, the paper concludes with a summary in Section 5, highlighting the main contributions and potential implications of the developed numerical method.

II. Arrhenius-type look-ahead traffic flow model

Nonlocal traffic flow equations are increasingly employed to quantitatively simulate the dynamic and rapidly changing interactions among vehicles, capturing the emergent behaviors that arise from complex, interdependent movements on the road. These models extend beyond local traffic dynamics to consider the influence of traffic conditions over a broader spatial extent, offering a more holistic view of traffic behavior and providing insights into the cascading effects of traffic congestion and variability in driver behavior.

We are particularly interested in exploring a sophisticated traffic flow model characterized by its nonlocal-concave-convex flux function [10]. This model diverges from traditional approaches by incorporating a flux function that transitions between concave and convex forms depending on traffic density. Such a model is adept at depicting a more nuanced representation of traffic flow, reflecting real-world phenomena where traffic conditions can rapidly shift from free-flowing to congested states.

The mathematical formulation of the model is given by the partial differential equation:

$$\partial_t \rho + \partial_x \left(f(\rho) \exp(-\kappa_\eta * \rho) \right) = 0, \tag{1}$$

where

$$f(\rho) = v_{\max} \rho (1-\rho)^\gamma, \quad \gamma > 1$$

and

$$\kappa_\eta * \rho(t,x) = \int_x^{x+\eta} \kappa_\eta (y-x) \rho(t,y) dy, \qquad \eta > 0.$$

The Kernel κ_η is a decreasing function such that

$$\kappa_\eta \in C^1([0,\eta];\mathbb{R}^+), \ \int_0^\eta \kappa_\eta(x)dx = 1,$$

$\rho(t,x)$ is the local traffic density, with $\rho \in [0, \rho_{\max}]$, $(t,x) \in \mathbb{R}^2$, $\rho_{\max}$ is the maximum density, $v_{\max}$ is a maximum traffic velocity, and f represents a fundamental diagram such that $f \in C^1(I;\mathbb{R}^+)$.

The model was first published in 2006 [16] by Sopasakis and Katsoulakis (SK), using $\kappa_\eta = 1$. An updated version was proposed in 2009 by Kurganov and Polizzi [9].

The model is an extension of one of the most well-known macroscopic traffic flow models, the Lighthill-Whitham-Richards (LWR) [11],

$$\partial_t \rho + \partial_x \left(\rho v(\rho) \right) = 0, \quad v(\rho) = v_{\max}(1-\rho). \tag{2}$$

The flux in (2) is concave and symmetric. However, statistical evidence from traffic networks in the real world indicates that neither a concave nor symmetric flux is expected. Instead, as the density increases, the measured empirical fluxes become right-skewed and convex, as seen in [8].

Another source of concern is the SK model's fundamental diagram (2). In contrast to the experimental results [8], the flux

$$f(\rho) = v_{\max} \rho (1-\rho) \tag{3}$$

is a concave function with even symmetry (concerning $\rho = \frac{1}{2}$). A flux that is right-skewed and non-concave seems to fit better.

$$f(\rho) = v_{\max} \rho (1-\rho)^\gamma, \qquad \gamma > 1. \tag{4}$$

The flux f in (4) has a right skew and changes from concave to convex at $\rho = \frac{2}{\gamma+1}$.

III. Numerical scheme

In this section, we provide a brief overview of the staggered Nessyahu-Tadmor (NT) schemes before presenting our unstaggered extension in one space dimension for numerically solving nonlocal conservation laws of the form [1].

$$\begin{cases} \partial_t \rho + \partial_x F(\rho, U) = 0, & x \in \mathbb{R},\, t > 0, \\ \rho(0,x) = \rho_0(x), & \rho_0 \in \text{BV}\left(\mathbb{R}, [0, \rho_{max}]\right), \end{cases} \tag{5}$$

where we define the convolution product as being:

$$U(t,x) = \kappa_\eta * \rho(t,x).$$

BV represents the space of functions with bounded variation., i.e.

$$\text{BV} = \{u \in L^1(\mathbb{R}) / \text{TV}(u) < \infty\},$$

with

$$\text{TV}(u) = \sup_{\varepsilon > 0} \frac{1}{\varepsilon} \int_{\mathbb{R}} |u(x+\varepsilon) - u(x)| dx.$$

A. Nessyahu-Tadmor scheme

We begin with a consistent subdivision of the computational domain. We define the control cells as $C_i = [x_{i-\frac{1}{2}}, x_{i+\frac{1}{2}}]$ is centered at the nodes x_i, of length Δx, and we designate by $D_{i+\frac{1}{2}}$ the dual cells $[x_i, x_{i+1}]$. We assume the numerical solution ρ_i^n of the equation $\rho_t + \partial_x F(\rho, U) = 0$ is known at time t^n at the nodes x_i, i.e.,

$$\rho_i^n = \frac{1}{\Delta x} \int_{x_{i-\frac{1}{2}}}^{x_{i+\frac{1}{2}}} \rho(t^n, x) dx.$$

The NT scheme calculates the solution $\rho_{i+\frac{1}{2}}^{n+1}$ at time t^{n+1} at the centers $x_{i+\frac{1}{2}}$ of the dual cells $[x_i, x_{i+1}]$ using the equation

$$\begin{aligned} \rho_{i+\frac{1}{2}}^{n+1} &= \frac{1}{2}(\rho_i^n + \rho_{i+1}^n) + \frac{\Delta x}{8}(\delta_i^n - \delta_{i+1}^n) \\ &- \lambda(F(\rho_{i+1}^{n+\frac{1}{2}}, U_{i+1}^{n+\frac{1}{2}}) - F(\rho_i^{n+\frac{1}{2}}, U_i^{n+\frac{1}{2}})), \quad \lambda = \frac{\Delta t}{\Delta x}, \end{aligned} \tag{6}$$

where

$$\delta_i^n = \frac{(\rho_i^n)'}{\Delta x} \simeq \frac{\partial \rho(t,x)}{\partial x} \rfloor_{x=x_0} + o(\Delta x)$$

is a limited numerical gradient that approximates the partial derivative to first-order accuracy; this leads to second-order spatial accuracy [7]. Second-order temporal accuracy is obtained thanks to a predictor-corrector step.

The time step t in Eq. (6) is dynamically calculated using the stability condition

$$\frac{\Delta t}{\Delta x} < \frac{1}{2\lambda_{\max}}, \quad \lambda_{\max} = \max_{\rho\in[0,\rho_{\max}]} \left|\frac{\partial F(\rho,U)}{\partial \rho}\right|.$$

Nessyahu and Tadmor [15] give a detailed description of the one-dimensional NT system.

One of the method's weaknesses is that the numerical solution in the NT-type schemes switches between two staggered grids at subsequent time steps. More specifically, any treatment of the updated solution typically requires the solution values computed at different previous times (e.g., at time t^n, t^{n-1}, and maybe earlier). A synchronization problem arises if the numerical solution obtained using an NT-type base scheme (at time t^{n+1}) requires additional treatment to satisfy a physical property. When the original and staggered grids' cells are different in shape or kind [13], the problem becomes considerably more difficult.

B. Unstaggered central scheme

We assume that the numerical solution ρ_i^n is known at time t^n at the nodes x_i, the solution at the next time, $t^{n+1} = t^n + \Delta t$ is computed in two steps, as follows [13]:

First, we obtain an estimate $\rho_{i+\frac{1}{2}}^{n+1}$ of the solution at time t^{n+1} on the dual cells $D_{i+\frac{1}{2}}$ using Nessyahu and Tadmor's formula (6) as follows:

$$\begin{aligned}\rho_{i+\frac{1}{2}}^{n+1} = \frac{1}{2}(\rho_i^n + \rho_{i+1}^n) + \frac{\Delta x}{8}(\delta_i^n - \delta_{i+1}^n) \\ - \lambda(F(\rho_{i+1}^{n+\frac{1}{2}}, U_{i+1}^{n+\frac{1}{2}}) - F(\rho_i^{n+\frac{1}{2}}, U_i^{n+\frac{1}{2}})).\end{aligned} \quad (7)$$

Thanks to the dual cells, the Riemann problems that arise at the interface $x_{i+\frac{1}{2}}$ can be avoided. Using a first-order Taylor expansion in time and the original equation (1), the expected values $\rho_i^{n+\frac{1}{2}}$ and $U_i^{n+\frac{1}{2}}$ at the intermediate time step $t^{n+\frac{1}{2}}$ in Eq. (7) are approximated as follows:

$$\begin{aligned}\rho(t^{n+\frac{1}{2}}, x_j) &= \rho(t^n, x_j) + \tfrac{\Delta t}{2}\rho_t(t^n, x_j) \\ &= \rho_i^n + \tfrac{\Delta t}{2}(-\partial_x F(\rho, U)\rfloor_{(t^n, x_i)}) \\ &= \rho_i^n - \tfrac{\lambda}{2}(F_i)' \\ &= \rho_i^{n+\frac{1}{2}}\end{aligned} \quad (8)$$

and

$$\begin{aligned}U(t^{n+\frac{1}{2}}, x_j) &= U(t^n, x_j) + \tfrac{\Delta t}{2}U_t(t^n, x_j). \\ &= U_j^n + \tfrac{\Delta t}{2}(U_j^n)' \\ &= U_j^{n+\frac{1}{2}}.\end{aligned} \quad (9)$$

We compute the convolution terms in (9) using the mid-point and the composite trapezoidal rule, and we obtain:

$$\begin{aligned}U_j^n =& U(t^n, x_j) \\ =& \int_{x_j}^{x_j+\eta} \rho(t^n, x)\,\kappa_\eta(x - x_j)\,dx \\ =& \int_{x_j}^{x_{j+1/2}} \rho(t^n, x)\,\kappa_\eta(x - x_j)\,dx \\ &+ \int_{x_{j+N-1/2}}^{x_{j+N}} \rho(t^n, x)\,\kappa_\eta(x - x_j)\,dx \\ &+ \sum_{k=1}^{N-1} \int_{x_{j+k-\frac{1}{2}}}^{x_{j+k+\frac{1}{2}}} \rho(t^n, x)\,\kappa_\eta(x - x_j)\,dx \\ =& \left[\kappa_\eta(0)\rho_j^n + \kappa_\eta(\frac{\Delta x}{2})\left(\rho_j^n + \delta_j\frac{\Delta x}{2}\right)\right]\frac{\Delta x}{4} \\ &+ \left[\kappa_\eta(\eta - \frac{\Delta x}{2})(\rho_{j+N}^n - \delta_{j+N}\frac{\Delta x}{2}) + \kappa_\eta(\eta)\rho_{j+N}^n\right]\frac{\Delta x}{4} \\ &+ \sum_{k=1}^{N-1} \Delta x\kappa_\eta(k\Delta x)\rho_{j+k}^n\end{aligned}$$

and

$$\begin{aligned}(U_j^n)' =& U_t(t^n, x_j) \\ =& \int_{x_j}^{x_j+\eta} \rho_t(t^n, x)\,\kappa_\eta(x - x_j)\,dx \\ =& -\int_{x_j}^{x_j+\eta} F_x(\rho(t^n, x), U(t^n, x))\,\kappa_\eta(x - x_j)dx \\ =& -\left[\kappa_\eta(x - x_j)\,F(\rho(t^n, x), U(t^n, x))\right]_{x_j}^{x_j+\eta} \\ &+ \int_{x_j}^{x_j+\eta} \kappa_\eta'(x - x_j)F(\rho(t^n, x), U(t^n, x))\,dx \\ =& \kappa_\eta(0)\,F_j^n - \kappa_\eta(\eta)F_{j+N}^n \\ &+ \left[\kappa_\eta'(0)F_j^n + \kappa_\eta'(\eta)F_{j+N}^n\right]\frac{\Delta x}{2} \\ &+ \sum_{k=1}^{N-1} \Delta x\kappa_\eta'(k\Delta x)F_{j+k}^n,\end{aligned}$$

in which F_{j+k}^n denotes $F\left(\rho_{j+k}^n, U_{j+k}^n\right)$

To avoid false oscillations in the numerical solution, the approximate flux derivatives $(F_j)'$ in Eq. (8) and the slope limiters δ_i^n in Eq. (6) are carefully computed with limiters [15]. The primary tool utilized in this work is a generalized minmod (mm)limiter [17], where the reconstruction's slope and the 1-dimensional case's flux derivatives are chosen as

$$\delta_i^n = mm(\theta\frac{\rho_i^n - \rho_{i-1}^n}{\Delta x}, \frac{\rho_{i+1}^n - \rho_{i-1}^n}{2\Delta x}, \theta\frac{\rho_{i+1}^n - \rho_i^n}{\Delta x}), \quad (10)$$

$$(F_i^n)' = mm(\theta\frac{F_i^n - F_{i-1}^n}{\Delta x}, \frac{F_{i+1}^n - F_{i-1}^n}{2\Delta x}, \theta\frac{F_{i+1}^n - F_i^n}{\Delta x}). \quad (11)$$

The parameter θ is set so that $1 \leqslant \theta \leqslant 2$, and the minmod limiter is specified as:

$$mm(a, b) = \frac{sgn(a) + sgn(b)}{2}.\min(|a|, |b|). \quad (12)$$

Subsequently, the updated solution found in the dual cells is returned to the original grid using the proposed UCS approach. The piecewise linear reconstructions of the solution values defined on the cells C_i (and $D_{i+\frac{1}{2}}$) are used to define the numerical solution; therefore, we first define

the piecewise linear reconstructions of the dual-cell solution values: $\rho^D_{i+\frac{1}{2}}$

$$\rho^D_{i+\frac{1}{2}}(t^{n+1},x)=\rho^{n+1}_{i+\frac{1}{2}}+\delta^{n+1}_{i+\frac{1}{2}}(x-x_{i+\frac{1}{2}}),\quad x\in[x_i,x_{i+1}] \tag{13}$$

where $\delta^{n+1}_{i+\frac{1}{2}}$ denotes a limited numerical gradient that approximates the spatial derivative $\frac{\partial\rho(x,t)}{\partial x}\rfloor_{x=x_{i+\frac{1}{2}}}$; it is chosen as [4]:

$$\delta^{n+1}_{i+\frac{1}{2}}=mm(\theta\frac{\rho^n_{j+\frac{1}{2}}-\rho^n_{j-\frac{1}{2}}}{\Delta x},\frac{\rho^n_{j+\frac{3}{2}}-\rho^n_{j-\frac{1}{2}}}{2\Delta x},\theta\frac{\rho^n_{j+\frac{3}{2}}-\rho^n_{j+\frac{1}{2}}}{\Delta x}),\theta\in[1,2], \tag{14}$$

we then define the solution values ρ^{n+1}_i at the center of the cell $[x_{i-\frac{1}{2}},x_{i+\frac{1}{2}}]$ using the formula:

$$\rho^{n+1}_i=\alpha\rho^D_{i-\frac{1}{2}}\left(t^{n+1},x_{i-\frac{1}{2}}+\beta\Delta x\right)+(1-\alpha)\,\rho^D_{i+\frac{1}{2}}\left(t^{n+1},x_{i+\frac{1}{2}}-\beta\Delta x\right). \tag{15}$$

The values of the parameters α and β in Eq. (15) range between 0 and 1/2. For the calculations presented in this work, we used the values $\alpha=1/2$ and $\beta=1/4$.

Eq.(15) is rewritten using (13) and (15) as

$$\rho^{n+1}_i=\left(\alpha\rho^{n+1}_{i-\frac{1}{2}}+(1-\alpha)\rho^{n+1}_{i+\frac{1}{2}}\right)+\beta\Delta x\left(\alpha\delta^{n+1}_{i-\frac{1}{2}}-(1-\alpha)\delta^{n+1}_{i+\frac{1}{2}}\right). \tag{16}$$

The one-dimensional unstaggered central scheme algorithm operates as follows, in brief:

1) Knowing the solution ρ^n_i at time t^n, we obtain an update $\rho^{n+1}_{i+\frac{1}{2}}$ of the solution on the dual cells using Eq. (7)
2) Computes the solution at time t^{n+1} on the original and unique grid using Eq. (16).

The suggested UCS scheme is second-order precise in both space and time, and it has the same stability criteria as the original NT.

IV. Numerical results

In this section, we study the performance of our proposed scheme by using several numerical tests with different choices of $f\in C^1([0,1];\mathbb{R}^+)$:

$$f(\rho)=v_{\max}\rho(1-\rho)^\gamma,\quad \gamma\in\{2,3\}$$

with $v_{\max}$=1 and $\rho_{\max}$=1, and kernels $\kappa_\eta\in C^1([0,\eta];\mathbb{R}^+)$:

constant:	$\kappa_\eta(x)=\frac{1}{\eta}$,
linear decreasing:	$\kappa_\eta(x)=\frac{2}{\eta}(1-\frac{x}{\eta})$,
nonlinear decreasing:	$\kappa_\eta(x)=\frac{3}{2\eta}(1-\frac{x^2}{\eta^2})$.

In all tests, the computational domain is [0, 1], the parameter $\theta=2$ and the Current-Friedrichs-Lewy (CFL) is 0.5. We impose periodic boundary conditions, i.e.,

$$\rho^n_m=\rho^n_0,\ \text{and}\ \rho^n_{i+m}=\rho^n_i\ \text{for}\ i=1,\dots,N$$

where $N=[\frac{\eta}{\Delta x}]$, $m=\frac{1}{\Delta x}$ and $t^n=n\Delta t$

We utilize the UCS scheme with a refined mesh to get a reference solution because we cannot compute an exact solution. The cell average's L1-error is provided as follows:

$$\mathrm{L}^1(\Delta x)=\|\rho^{\Delta x}(t,x)-\rho^{\frac{\Delta x}{2}}(t,x)\|_{\mathrm{L}^1}$$

where $\rho^{\Delta x}(t,x)$ and $\rho^{\frac{\Delta x}{2}}(t,x)$ are the solutions computed with m and 2m mesh cells, respectively.

The numerical order of convergence is computed by

$$\delta(\Delta x)=\frac{\ln\left(\frac{\mathrm{L}^1(\Delta x)}{\mathrm{L}^1(\frac{\Delta x}{2})}\right)}{\ln(2)}$$

A. Test 1: Convergence to reference solution

We consider equation (1) subject to the following initial conditions including two constant states, as considered in [2]:

$$\rho_0(x)=\begin{cases}0.8, & \text{if}\quad 1/3<x<2/3,\\ 0.2, & \text{otherwise.}\end{cases} \tag{17}$$

We apply the UCS scheme to the problem (1), (17) and compute its solutions for the look-ahead distance η equals 0.1 at time t=0.11. The solutions, computed on two uniform grids with $\Delta x=1/80$ and $\Delta x=1/320$, together with the reference solution, obtained by the UCS scheme on a much finer uniform mesh with $\Delta x=1/1280$, are plotted in Figs. 1a, 1b, 1c, 2a, 2b and 2c. Compared to the reference solution, the numerical solutions derived using the UCS approach converge nicely to the reference solution.

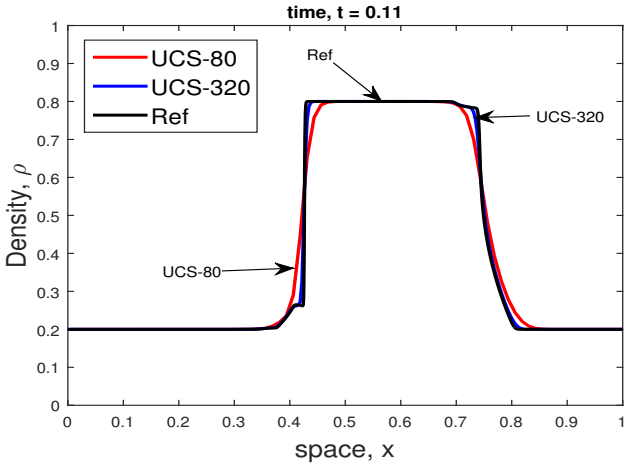

(a) $\kappa_\eta=\frac{1}{\eta}$

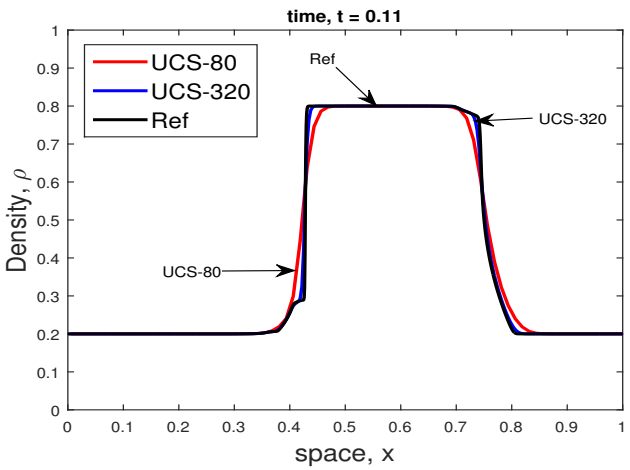

(b) $\kappa_\eta(x)=\frac{2}{\eta}(1-\frac{x}{\eta})$

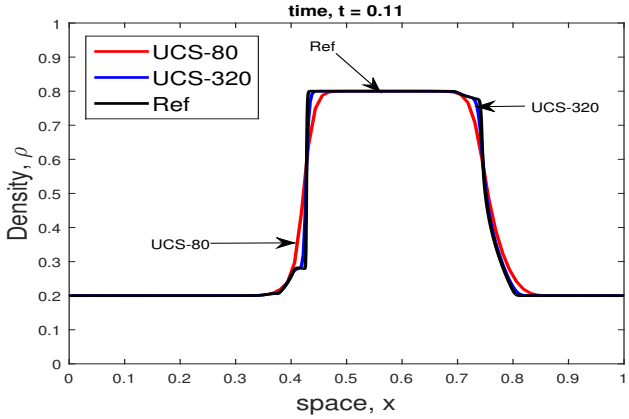

(c) $\kappa_\eta(x) = \frac{3}{2\eta}(1 - \frac{x^2}{\eta^2})$

Fig. 1. Comparison of solutions computed with the UCS scheme using $\gamma = 2$.

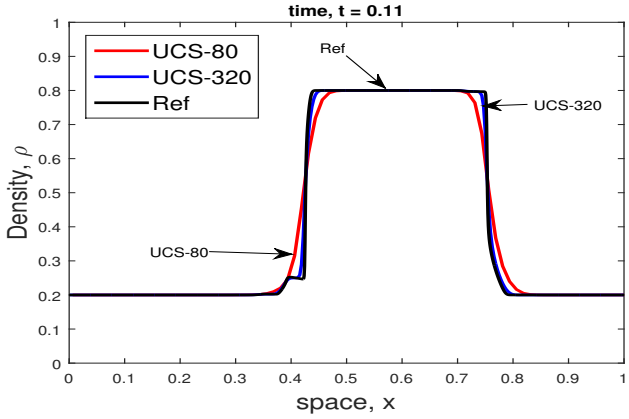

(a) $\kappa_\eta = \frac{1}{\eta}$

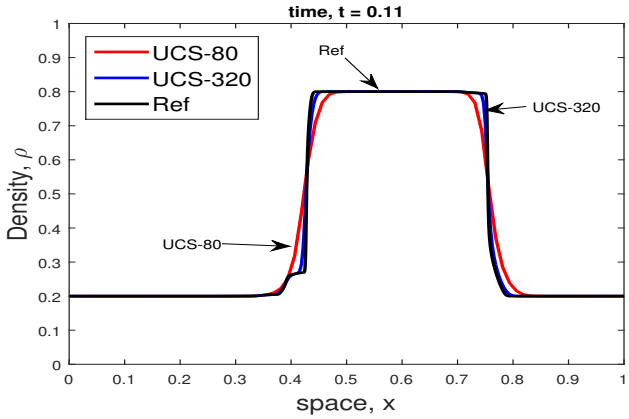

(b) $\kappa_\eta(x) = \frac{2}{\eta}(1 - \frac{x}{\eta})$

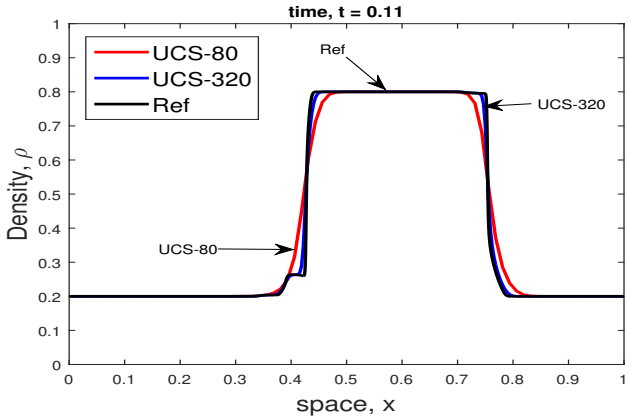

(c) $\kappa_\eta(x) = \frac{3}{2\eta}(1 - \frac{x^2}{\eta^2})$

Fig. 2. Comparison of solutions computed with the UCS scheme using $\gamma = 3$.

B. Test 2: Accuracy of the UCS scheme

To prove that the suggested approach in this work is second-order accurate, we consider a test case with a smooth function.

$$\rho_0(x) = 0.5 + 0.4\sin(\pi x) \tag{18}$$

We compare the L^1 errors and the convergence order of the UCS scheme with the NT scheme to show the precision and effectiveness of the UCS scheme. We fix $\eta = 0.1$, $f(\rho) = \rho(1-\rho)^2$, and the final time T=0.25. We contrast the L^1 of the corresponding numerical schemes on a uniform grid with $\Delta x = 1/320$ compared to a reference solution computed with the NT scheme and $\Delta x = 1/1280$. The spatial step size is given by $\Delta x = 0.1 \times 2^{-p}$ with $p \in \{2, ...6\}$. Table I provides the results of this test case. We observe that the correct order of convergence has been obtained for the UCS and NT schemes, and the L^1-errors obtained are nearly identical.

TABLE I
L^1 ERRORS AND CONVERGENCE ORDERS AT T=0.25

		UCS		NT	
κ_η	p	L^1error	$\delta(\Delta x)$	L^1error	$\delta(\Delta x)$
$\frac{1}{\eta}$	2	6,6087e-05	-	6,2733e-05	-
	3	1,6509e-05	2,00	1,5904e-05	1,97
	4	4,1506e-06	1,99	3,9621e-06	2,00
	5	1,0422e-06	1,99	9,8701e-07	2,00
	6	2,5964e-07	2,00	2,4611e-07	2,00
$\frac{2}{\eta}(1 - \frac{x}{\eta})$	2	7,0635e-05	-	6,6678e-05	-
	3	1,7439e-05	2,01	1,6879e-05	1,98
	4	4,3739e-06	1,99	4,2430e-06	1,99
	5	1,0976e-06	1,99	1,0611e-06	1,99
	6	2,7381e-07	2,00	2,6463e-07	2,00
$\frac{3}{2\eta}(1 - \frac{x^2}{\eta^2})$	2	7,2210e-05	-	6,8336e-05	-
	3	1,7851e-05	2,01	1,7324e-05	1,97
	4	4,4922e-06	1,99	4,3681e-06	1,98
	5	1,1323e-06	1,98	1,0913e-06	2,00
	6	2,8271e-07	2,00	2,7264e-07	2,00

C. Test 3: Limit $\eta \longrightarrow 0$

Here, we examine the limit situation $\eta \longrightarrow 0$ and quantitatively examine if the approximate solutions generated by the suggested unstaggered central scheme converge to the local traffic model solution.

$$\partial_t\rho + \partial_x\left(f(\rho)\exp(-\rho)\right) = 0,\ f(\rho) = v_{\max}\rho(1-\rho)^\gamma,\ \gamma > 1. \tag{19}$$

We take a numerical look at the same (non-linear) scenario as previously, but we vary $\eta \in \{0.1, 0.05, 0.025\}$ and use a fixed space step size $\Delta x = 1/320$. Consider the final time to be T = 1.15.

We calculate the L^1 distances between the approximate solutions produced by the suggested unstaggered central scheme used to (5) and the outcome for the related local problem (19) to assess the convergence. The corresponding L^1 distances shown in Table II decrease when η is small enough. The results are further illustrated in more detail in Figs. 3a, 3b, 3c, 4a, 4b and 4c.

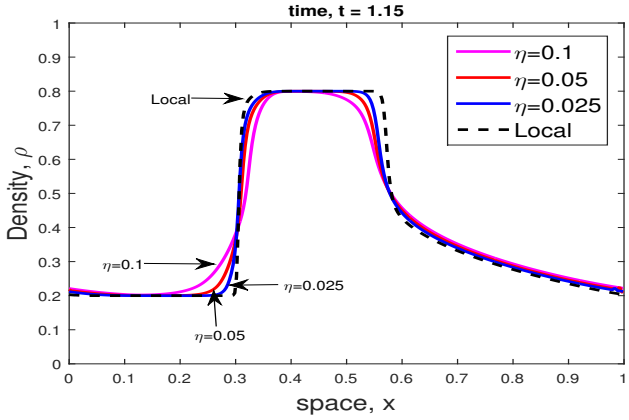

(a) $\kappa_\eta = \frac{1}{\eta}$

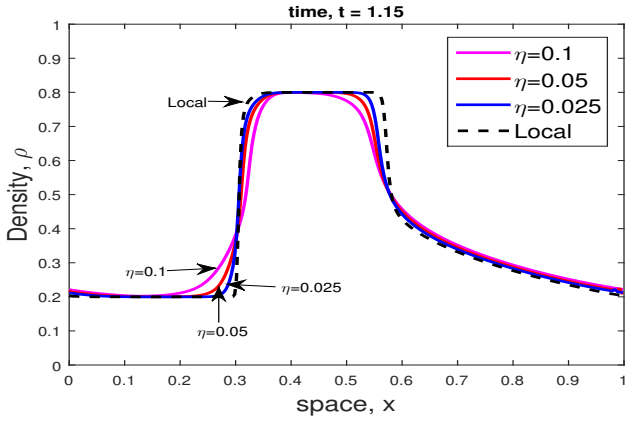

(b) $\kappa_\eta(x) = \frac{2}{\eta}(1 - \frac{x}{\eta})$

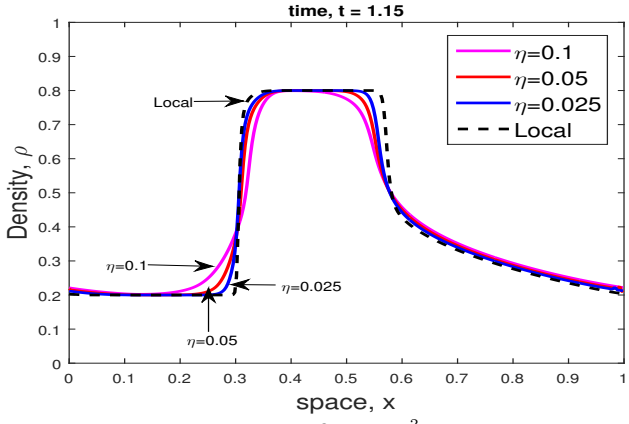

(c) $\kappa_\eta(x) = \frac{3}{2\eta}(1 - \frac{x^2}{\eta^2})$

Fig. 3. The solutions to the model (5) and non-local model (19), which were calculated using various kernel functions and decreasing values of $\eta = 0.1, 0.05, 0.025$ at T = 1.15 for $\gamma = 2$

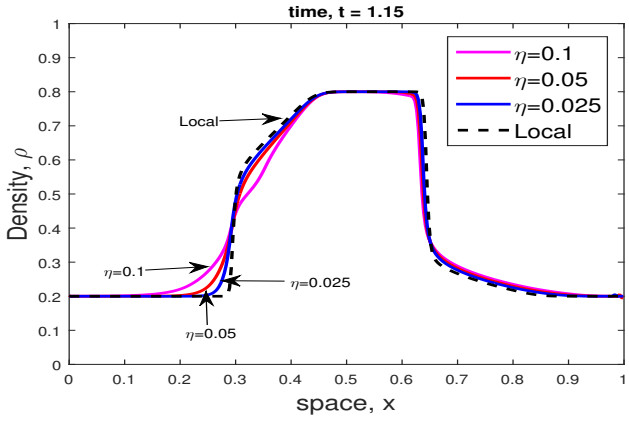

(a) $\kappa_\eta = \frac{1}{\eta}$

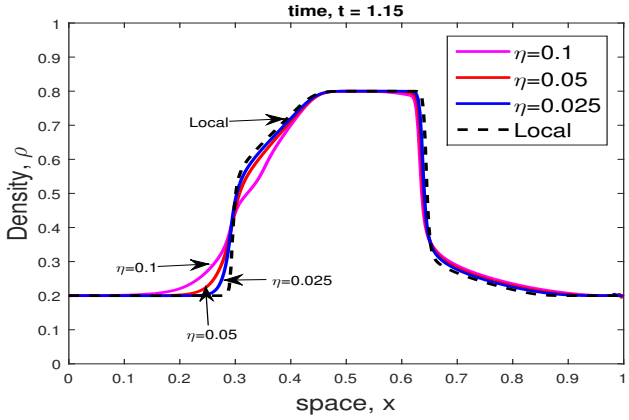

(b) $\kappa_\eta(x) = \frac{2}{\eta}(1 - \frac{x}{\eta})$

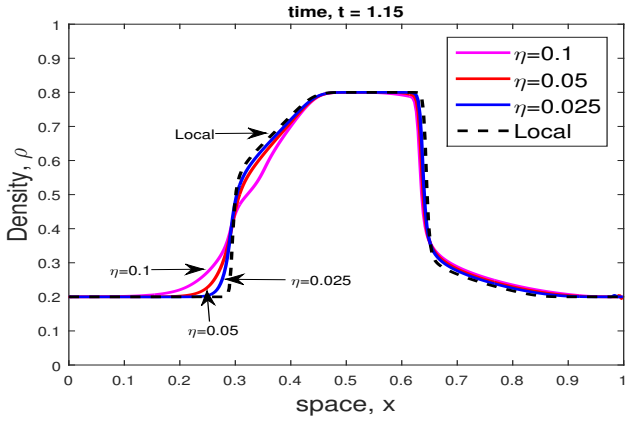

(c) $\kappa_\eta(x) = \frac{3}{2\eta}(1 - \frac{x^2}{\eta^2})$

Fig. 4. The solutions to the model (5) and non-local model (19), which was calculated using various kernel functions and decreasing values of $\eta = 0.1, 0.05, 0.025$ at T = 1.15 for $\gamma = 3$

TABLE II
L^1 DISTANCE BETWEEN THE APPROXIMATE SOLUTIONS TO THE LOCAL MODEL (19) AND THE NON-LOCAL MODEL (5)WITH KERNEL $\kappa_\eta(x) = \frac{2}{\eta}(1 - \frac{x}{\eta})$ FOR DIFFERENT VALUES OF η AT T = 1,15.

η	0.1	0.05	0.025
L^1 distance	0.0578	0.0343	0.0204

In the case of the Arrhenius look-ahead model, as shown in Figs. 3a, 3b, 3c, 4a, 4b, and 4c the solutions to the non-local model (5) equation appear to converge to the solution of the local model (19) equation as the look-ahead distance converges to 0. As one can see, the dependence on η is evident; thus, the non-local flux has a negligibly small effect as η decreases.

D. Test 4: Comparison of the schemes NT and UCS

Here, we aim to compare the approximate solutions with the original NT and UCS schemes. For this purpose, we set the initial conditions to be (17) in Figs. 5a, 5b, 5c, 6a, 6b, and 6c, we depict the solutions that arise from the two choices of γ. We can see from Figs. 5a, 5b, 5c, 6a, 6b, and 6c that there is a good agreement between the NT scheme and the proposed scheme, thus confirming the efficiency and the potential of our proposed unstaggered central scheme.

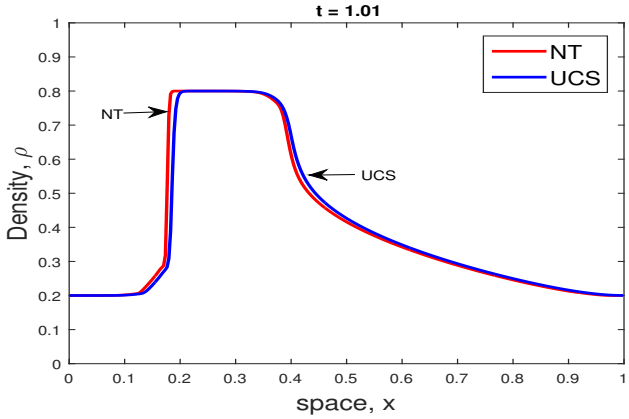

(a) $\kappa_\eta = \frac{1}{\eta}$

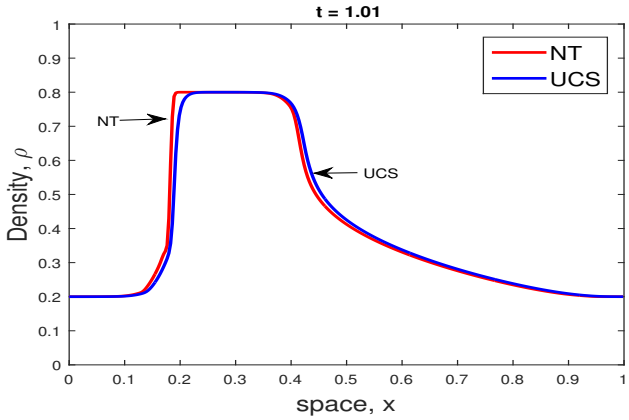

(b) $\kappa_\eta(x) = \frac{2}{\eta}(1 - \frac{x}{\eta})$

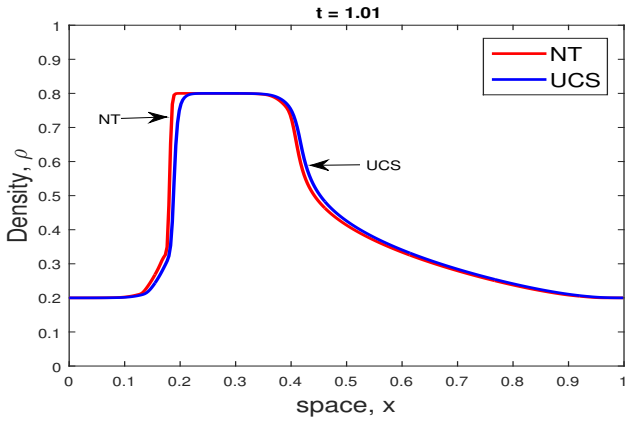

(c) $\kappa_\eta(x) = \frac{3}{2\eta}(1 - \frac{x^2}{\eta^2})$

Fig. 5. Comparison of the UCS and NT scheme for $f(\rho) = \rho(1-\rho)^2$, at $T = 1.01$

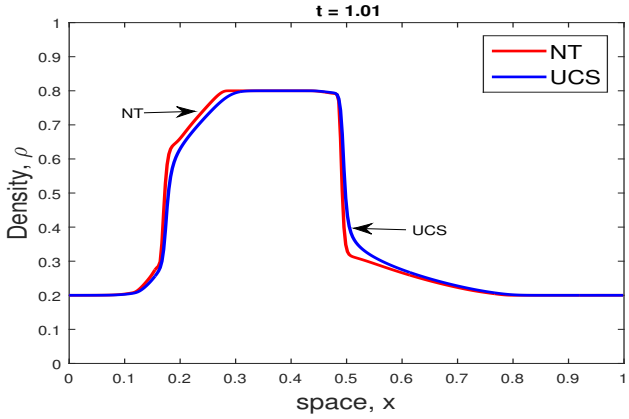

(a) $\kappa_\eta = \frac{1}{\eta}$

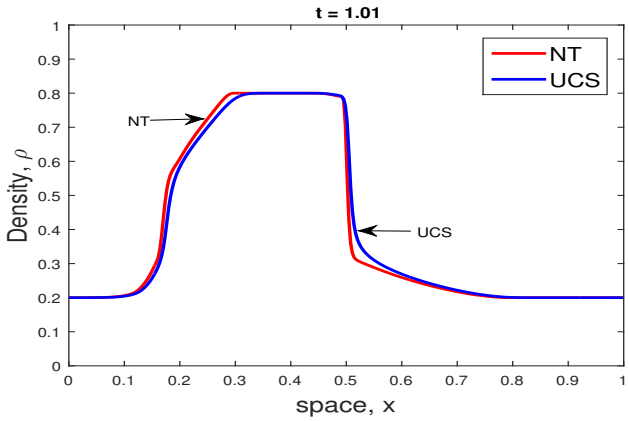

(b) $\kappa_\eta(x) = \frac{2}{\eta}(1 - \frac{x}{\eta})$

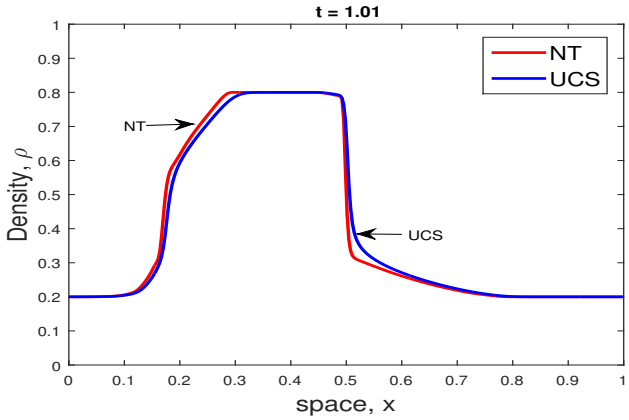

(c) $\kappa_\eta(x) = \frac{3}{2\eta}(1 - \frac{x^2}{\eta^2})$

Fig. 6. Comparison of the UCS and NT schemes for $f(\rho) = \rho(1-\rho)^3$ at $T = 1.01$

V. Conclusion

In this study, we have introduced and evaluated an unstaggered central scheme for numerically solving nonlocal conservation laws, specifically tailored for traffic flow models with Arrhenius-type look-ahead rules. Our developed method leverages a second-order accurate finite volume approach that operates on a single computational grid, thereby simplifying the computation and potentially increasing efficiency by avoiding the complexities of staggered grids typically used in traditional schemes. The scheme that was developed as a result is an accurate scheme of the second order in both space and time. It develops a piecewise linear numerical solution and avoids the resolution of the Riemann problems that occur at the cell interfaces. Following this, the suggested numerical technique is verified for a nonlocal traffic model with a concave-convex flux distribution.

The efficiency of these numerical tools is validated by extensive numerical experiments showing capability in handling nonlocal traffic flow models while keeping essential features of accuracy and non-oscillatory properties. The consistency of results, with good alignment with the established literature, proves our method's robustness and applicability.

This work helps to provide more efficient numerical tools for the simulation of traffic flow and helps in understanding nonlocal traffic dynamics. It opens a way for future research to further extend this methodology to even more complicated and realistic models of traffic and thus further enrich the current discipline of traffic modeling.

REFERENCES

[1] S. Belkadi, M. Atounti, "A class of Central Unstaggered Schemes for Nonlocal Conservation Laws: Applications to Traffic Flow Models," *Boletim da Sociedade Paranaense de Matematica*, vol. 42, pp. 1–12, 2024.

[2] S. Belkadi, M. Atounti, "Non-oscillatory central schemes for general nonlocal traffic flow models," *International Journal of Applied Mathematics*, vol. 35, no. 4, pp. 515–528, 2022.

[3] S. Belkadi, M. Atounti, "Central Finite Volume Schemes for Non-Local Traffic Flow Models with Arrhenius-type Look-Ahead Rules," *Mathematical Modeling and Computing*, vol. 10, no. 4, pp. 1100–1108, 2023.

[4] S. Belkadi, M. Atounti, "Unstaggered central schemes for one-dimensional nonlocal conservation laws," *International Journal of Applied Mathematics*, vol. 37, no. 2, pp. 155–164, 2024.

[5] P. Goatin, S. Scialanga, "Well-posedness and finite volume approximations of the LWR traffic flow model with non-local velocity," *Networks and Heterogeneous Media*, vol. 11, no. 1, pp. 107–121, 2016.

[6] S. Jenjira, P. Nopparat, "A Mathematical Model for Evaluating the Risk of Airborne Infection Among Bus Passengers Using Ventilation Systems," *IAENG International Journal of Applied Mathematics*, vol. 54, no. 2, pp. 169-176, 2024.

[7] G. Jiang, E. Tadmor, "Non-oscillatory central schemes for multidimensional hyperbolic conservation laws," *SIAM Journal on Scientific Computing*, vol. 19, pp. 1892–1917, 1998.

[8] R. D. Kuhne, N. H. Gartner, "75 Years of the Fundamental Diagram for Traffic Flow Theory: Greenshields Symposium," *Transportation Research Board E-Circular*, 2011.

[9] A. Kurganov, A. Polizzi, "Non-oscillatory central schemes for a traffic flow model with Arrhenius look-ahead dynamics," *Networks and Heterogeneous Media*, vol. 4, no. 3, pp. 431–451, 2009.

[10] Y. Lee, "Thresholds for shock formation in traffic flow models with nonlocal concave-convex flux," *Journal of Differential Equations*, vol. 266, no. 1, pp. 580–599, 2019.

[11] M. Lighthill, G. B. Whitham, "On kinematic waves. II. A theory of traffic flow on long, crowded roads," *Proceedings of the Royal Society A*, vol. 229, pp. 317–345, 1995.

[12] S. Mingyang, T. Ying, "Research on Traffic Sign Object Detection Algorithm Based on Deep Learning," *Engineering Letters*, vol. 32, no. 8, pp. 1562-1568, 2024.

[13] R. Touma, "Central unstaggered finite volume schemes for hyperbolic systems: Applications to unsteady shallow water equations," *Applied Mathematics and computation*, vol. 213, no. 1, pp. 47-59, 2009.

[14] R. Touma, "Unstaggered central schemes with constrained transport treatment for ideal and shallow water magnetohydrodynamics," *Applied Mathematics and computation*, vol. 60, no. 7, pp. 752-766, 2010.

[15] H. Nessyahu, E. Tadmor, "Non-oscillatory central differencing for hyperbolic conservation laws," *Journal of Computational Physics*, vol. 87, no. 2, pp. 408–463, 1990.

[16] A. Sopasakis, M. A. Katsoulakis, "Stochastic modeling and simulation of traffic flow: asymmetric single exclusion process with Arrhenius look-ahead dynamics," *SIAM Journal on Applied Mathematics*, vol. 66, no. 3, pp. 921-944, 2006.

[17] B. Van Leer, "Towards the ultimate conservative difference scheme V. A second-order sequel to Godunov's method," *Journal of Computational Physics*, vol. 32, pp. 101–136, 1979.